

Influence of external temperature gradient on acoustoelectric current in graphene

K. A. Dompreeh^{a,1,*}, N. G. Mensah^b, S. Y. Mensah^a, R. Edziah^a

^a*Department of Physics, College of Agriculture and Natural Sciences, U.C.C, Ghana.*

^b*Department of Mathematics, College of Agriculture and Natural Sciences, U.C.C, Ghana*

Abstract

Recent analyses of thermoelectric amplification of acoustic phonons in Free-Standing Graphene (FSG) Γ_q^{grap} have prompted the theoretical study of the influence of external temperature gradient (∇T) on the acoustoelectric current $j_T^{(grap)}$ in FSG. Here, we calculated thermal field on open circuit ($j_T^{(grap)} = 0$) to be $(\nabla T)^g = 746.8 Km^{-1}$. We then calculated acoustoelectric current ($j_T^{(grap)}$) to be $1.1mA\mu m^{-2}$ for $\nabla T = 750.0 Km^{-1}$, which is comparable to that obtained in semiconductors ($1.0mA\mu m^{-2}$), the thermal-voltage $(V_T)_0^g$ to be $6.6\mu V$ and the Seebeck coefficient S as $8.8\mu V/K$. Graphs of the normalized $j_T^{(grap)}/j_0$ versus ω_q , T and $\nabla T/T$ were sketched. For $j_T^{(grap)}$ on T for varying ω_q , Negative Difference Conductivity (NDC) ($|\frac{\partial j}{\partial T}| < 0$) was observed in the material. This indicates graphene is a suitable material for developing thermal amplifiers and logic gates.

Keywords: acoustoelectric , graphene, temperature gradient, Negative Differential Conductivity

*Corresponding author

Email: kwadwo.dompreeh@ucc.edu.gh

This work is licensed under the Creative Commons Attribution International

License (CC BY). <http://creativecommons.org/licenses/by/4.0/>

Introduction

The ability to acoustically generate d.c current in bulk and low dimensional materials such as Superlattices (SL) [1, 2, 3, 4], Carbon Nanotubes (CNTs) [5, 6, 7, 8] and Quantum wires (QW) [9, 10] have recently become an active field of study. This phenomena is known as Acoustoelectric Effect (AE) and is caused by the attenuation of phonons leading to the appearance of a dc field. In Graphene, this effect has been verified theoretically [11, 12, 13] and experimentally [14, 15, 16, 17]. The high intrinsic carrier mobility (over $2 \times 10^5 \text{cm}^2/\text{Vs}$) of a 2-D graphene sheet, coupled with its amazingly high value for thermal conductivity at room temperatures ($\approx 3000 - 5000 \text{W/mK}$), causes substantial acoustic effect when there is a minimal change in the external temperature gradient (∇T) [18]. This could lead to activities such as AE [19], amplification of acoustic phonons [20] or Acoustomagnetolectric effect (AME) in the sample [21, 22]. The influence of non-linear thermal transport in graphene has received little attention as against other non-linear effects such as electric and magnetic fields which are utilised in ideal atomic chains [24, 25, 26, 27], molecular junctions [28] and quantum dots [29]. Daschewski et. al [33], treated the influence of energy density fluctuations (EDFs) on thermo-acoustic sound generation for near-field effects and sound-field attenuation for AirTech 200, UltranGN-55 and thermo-acoustic transducer. Hu et. al. [30] employed classical molecular dynamics to study the non-linear transport in Graphene Nanoribbons (GNRs). The Negative Differential Thermal Conductivity (NTDC) obtained by using the LAMMPS (Large-scale Atomis/ Molecular Massively Parallel Simulator)

package and velocity scaling software vanishes for lengths $> 50nm$ long GNR. Such studies have particular applications in thermal power sources such as thermophones, plasma firings and laser beams [30] but till date there is no theoretical study of the influence of ∇T on acoustoelectric effect in Graphene.

In FSG, there are two types of phonons: (1) in-plane phonons with linear and longitudinal acoustic branches (LA and TA); and (2) out-of-plane phonons known as flexural phonons (ZA and ZO) [32]. In this paper, we consider a stretched FSG in which flexural phonons are ignored and only in-plane phonons couples linearly to electrons. This study is done in the hypersound regime having $ql \gg 1$ (where q is the acoustic phonon wavenumber, l is the electron mean-free path). Here, Negative Differential Conductivity (NDC) in FSG is reported. This is analogous to the electronic NDC [33, 34] which is a useful ingredient for developing graphene based thermal systems such as signal manipulation devices, thermal logic gates and thermal amplifiers [31].

The paper is organised as follows: In the theory section, the equation underlying the acoustoelectric effect in graphene is presented. In the numerical analysis section, the final equation is analysed and presented in a graphical form. Lastly, the discussion and conclusions are presented.

Theory

The acoustoelectric current (j_T) generated in a graphene sheet can be expressed as [24, 25]

$$j_T = -\frac{e\tau A|C_q|^2}{(2\pi)^2 V_s} \int_0^\infty k dk \int_0^\infty k' dk' \int_0^{2\pi} d\phi \int_0^{2\pi} d\theta \{ [f(k) - f(k')] \times \\ V_i \delta(k - k' - \frac{1}{\hbar V_F}(\hbar\omega_q)) \} \quad (1)$$

From [26], the matrix element $|C_q|$ in Eqn.(1) is given as

$$|C_q| = \begin{cases} \sqrt{\frac{\Lambda^2 \hbar q^2}{2\rho\omega_q}} & \text{acoustic phonons} \\ \sqrt{[(\frac{2\pi^2\rho\omega_0}{q^2})(k_\infty^{-1} - k_0^{-1})]} & \text{optical phonons} \end{cases}$$

where, Λ is the constant of deformation potential, ρ is the density of the graphene sheet, τ is the relaxation constant, V_s is the velocity of sound, A is the area of the graphene sheet, ω_0 is the frequency of an optical phonon, k_∞^{-1} and k_0^{-1} are the low frequency and optical permeability of the crystal. The linear energy dispersion at the Fermi level with low-energy excitation is $\varepsilon(k) = \pm\hbar V_F|k|$ (the Fermi velocity $V_F \approx 10^8 \text{ms}^{-1}$). From Eqn.(1), the velocity V_i is given as $v(k) = \partial\varepsilon(k)/\hbar\partial k$ (where $V_i = v(k') - v(k)$) yields

$$V_i = \frac{2\hbar\omega_q}{\hbar V_F} \quad (2)$$

From Eqn.(1), the linear approximation of the distribution function $f(k)$ is given as

$$f(k) = f_0(\varepsilon(k)) + f_1(\varepsilon(k)) \quad (3)$$

The unperturbed electron distribution function is given by the shifted Fermi-Dirac function,

$$f_0(k) = \{\exp(\beta\varepsilon(k) - \beta\varepsilon_F) + 1\}^{-1} \quad (4)$$

where $\beta = 1/k_B T$ (k_B is the Boltzmann's constant and T is the absolute temperature), and ε_F is the Fermi energy. At low temperatures, $\varepsilon_F = \xi$ (ξ is the chemical potential) and the Fermi-Dirac equilibrium distribution function become

$$f_0(\varepsilon(k)) = \exp(-\beta(\varepsilon(k) - \xi)) \quad (5)$$

From Eqn. (3), $f_1(k)$ is derived from the Boltzmann transport equation as

$$f_1(\varepsilon(k)) = \tau[(\varepsilon(k) - \xi) \frac{\nabla T}{T}] \frac{\partial f_0(p)}{\partial \varepsilon} v(k) \quad (6)$$

Here τ is the relaxation time, and ∇T is the temperature gradient. With $k' = k - \frac{1}{\hbar V_F}(\hbar \omega_q)$, and inserting Eqn.(2), (3),(5) and (6) into Eqn.(1) and expressing further gives

$$j_T = \frac{-eA|\Lambda|^2 \hbar q \tau}{(2\pi)V_F \rho V_s} \int_0^\infty (k^2 - \frac{k\omega_q}{V_F}) \{ \exp(-\beta(\hbar V_F k)) - \beta V_F q \tau (\hbar V_F k) \times \\ \frac{\nabla T}{T} \exp(-\beta \hbar V_F k) - \exp(-\beta \hbar V_F (k - \frac{\omega_q}{V_F})) - \beta \hbar V_F \tau (\hbar V_F (k - \frac{\omega_q}{V_F})) \times \\ \frac{\nabla T}{T} \exp(-\beta \hbar V_F (k - \frac{\omega_q}{V_F})) \} dk \quad (7)$$

Using standard integrals and after some cumbersome calculations, Eqn(7) yields the current (j_T) as

$$j_T = j_0 \{ (2 - \beta \hbar \omega_q) (1 - \exp(-\beta \hbar \omega_q)) \\ - \tau V_F [6(1 + \exp(\beta \hbar \omega_q)) - \beta \hbar \omega_q (2 + \beta \hbar \omega_q \exp(\beta \hbar \omega_q))] \frac{\nabla T}{T} \} \quad (8)$$

where

$$j_0 = \frac{-2eA\tau|\Lambda|^2 q}{2\pi\beta^3 \hbar^3 V_F^4 \rho V_s} \quad (9)$$

From Eqn.(8), for an open circuit ($j_T = 0$), the thermal field $(\nabla T)^g$ is calculated as

$$(\nabla T)^g = T \frac{\{(2 - \beta \hbar \omega_q) (1 - \exp(-\beta \hbar \omega_q))\}}{\tau V_F [6(1 + \exp(\beta \hbar \omega_q)) - \beta \hbar \omega_q (2 + \beta \hbar \omega_q \exp(\beta \hbar \omega_q))]} \quad (10)$$

the thermal field $(\nabla T)^g$ is found to depend on the temperature (T), the frequency (ω_q) and the relaxation time (τ) as well as the acoustic wavenumber

(q). The threshold temperature gradient $(\nabla T)^g$ relate the thermal voltage $V_T = k_\beta T/e$ as

$$(\nabla V)_T = -S(\nabla T)^g \quad (11)$$

where the Seebeck coefficient (S) is given as

$$S = \frac{k_\beta \{ \tau V_F [6(1 + \exp(\beta \hbar \omega_q)) - \beta \hbar \omega_q (2 + \beta \hbar \omega_q \exp(\beta \hbar \omega_q))] \}}{e(2 - \beta \hbar \omega_q)(1 - \exp(-\beta \hbar \omega_q))} \quad (12)$$

Numerical Analysis

To analyse, Eqn. (8), (9) and (12), we used the the following parameters: $\Lambda = 9eV$, $V_s = 2.1 \times 10^3 ms^{-1}$, $\tau = 5 \times 10^{-10}s$, $\omega_q = 10^{12}s^{-1}$ and $q = 10^4 m^{-1}$. At $T = 77K$, the thermal field generated on open circuit $(\nabla T)^g$ is calculated to be $746.8Km^{-1}$. To clarify the results obtained, the dependence of the normalized acoustoelectric current j_T/j_0 on ω_q , T , q and $\nabla T/T$ are analysed graphically. In Figure 1a, the dependence of $j_T^{(grap)}/j_0$ on ω_q for varying ∇T are presented. We observed that at $\nabla T = 850Km^{-1}$, the graph rises to a maximum at $j_T^{(grap)}/j_0 = 2.8$ then decreased. By decreasing ∇T to $500Km^{-1}$, the graph decreases to a minimum at $j_T^{(grap)}/j_0 = -0.8$ and then increases. Figure 1b shows the temperature dependence on the normalized acoustoelectric current $j_T^{(grap)}/j_0$ for various ω_q . We observed that for increasing temperatures, the graph raises to a peak value and then decreases. The region of the decrease (negative slope) indicates Negative Differential Conductivity (NDC) ($|\frac{\partial j}{\partial T}| < 0$) in the materials. The peak values increases with increases in ω_q . In Figure 2, the behaviour of $j_T^{(grap)}/j_0$ versus $\nabla T/T$ for varying ω_q and q are presented. For Figure 2, it was noted that the graphs initially attained minimum points then increase for increasing $\nabla T/T$ to a maximum point then falls off. It is observed that the ratio of the absolute value of the

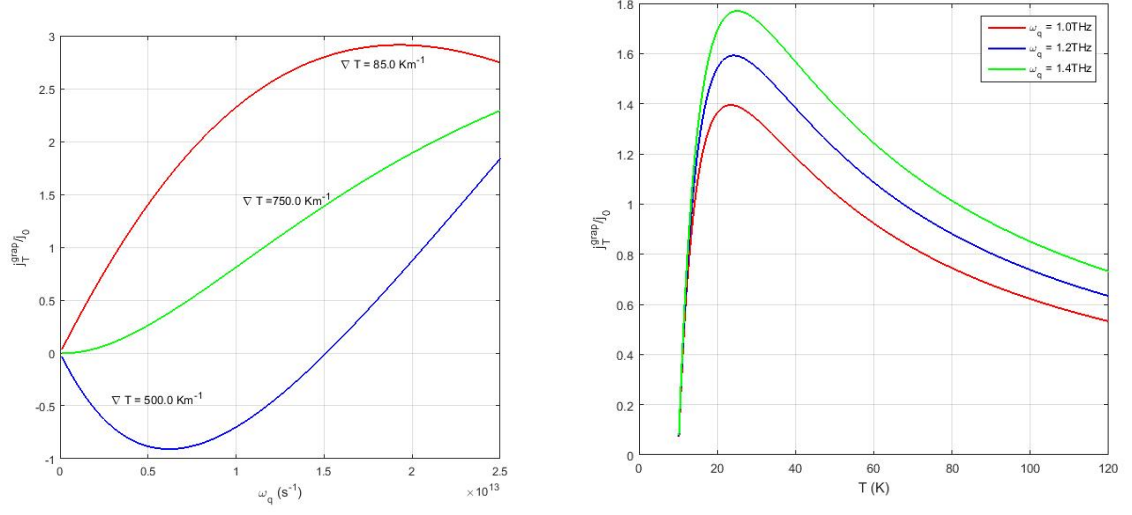


Figure 1: (a) Dependence of $j_T^{(grap)}/j_0$ on ω_q , (b) a graph of $j_T^{(grap)}/j_0$ on $T(K)$

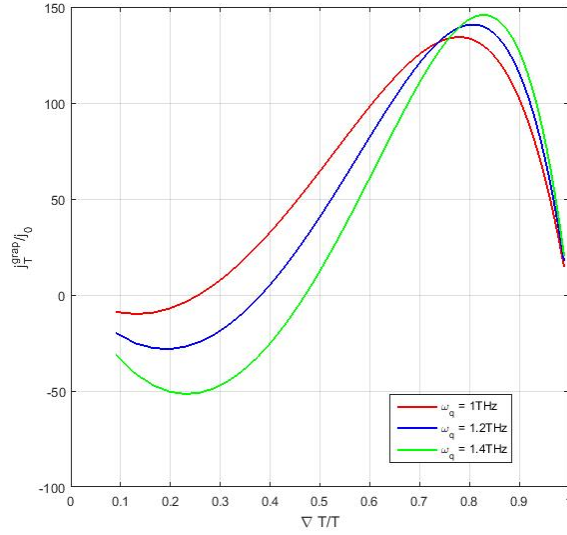


Figure 2: the dependence of $j_T^{(grap)}/j_0$ versus $\nabla T/T$ for varying ω_q .

maximum peak $|j_T^{(grap)}/j_0|_{max}$ to the minimum $|j_T^{(grap)}/j_0|_{min}$ peak is quite big. In the case where $\omega_q = 1.4THz$, the ratio $\frac{|j_T^{(grap)}/j_0|_{max}}{|j_T^{(grap)}/j_0|_{min}} \approx 3$. A similar observation was made in superlattice for the case of electric field [4]. A 3D plot of the dependence of the normalized acoustoelectric current $j_T^{(grap)}/j_0$ on ω_q and q are presented in Figure 3a and b. The current density ($j_T^{(grap)}$) gen-

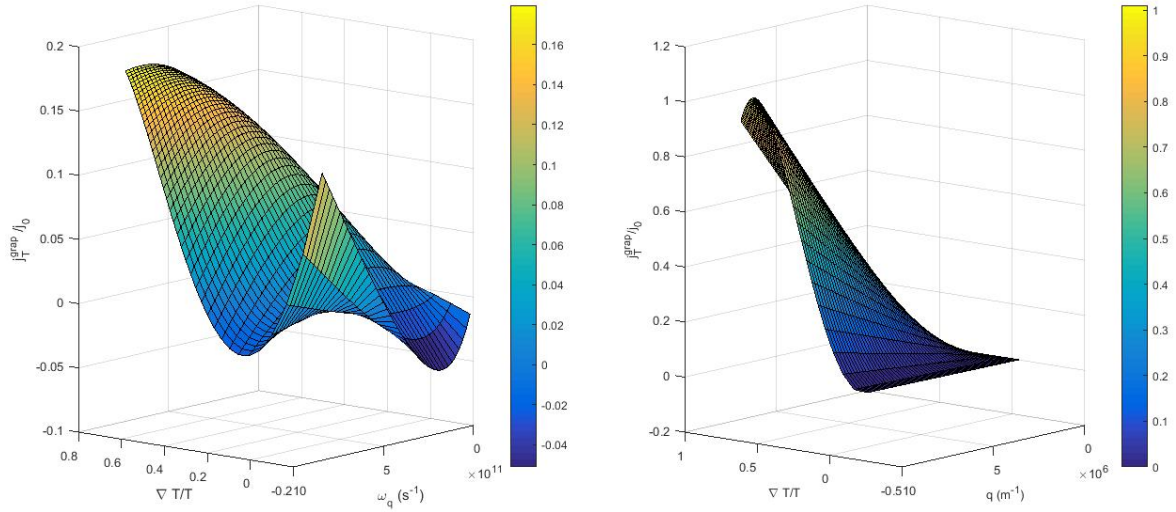


Figure 3: (a) the dependence of $j_T^{(grap)}/j_0$ versus $\nabla T/T$ on ω_q (a) the dependence of j_T/j_0 versus $\nabla T/T$ on q

erated per unit area in the sample at $\omega_q = 0.1THz$ and $\nabla T = 750.0Km^{-1}$ is calculated to be $j_T^{(grap)} = 1.1mA(\mu m)^{-2}$ as compared to that calculated in semiconductors ($\approx 1.0mA(\mu m)^{-2}$). Eqn.(12) is the Seebeck coefficient S which deals with the main thermoelectric properties of the FSG and how efficient it is. Fig. 4a shows the dependence of S on ω_q for various $\nabla T/T$. The asymmetric distribution is due to electrons moving at the Fermi level in the material with an energy related to the Fermi energy. The value of S ranges from $152\mu V/K$ to $-22.7\mu V/K$ at $\nabla T/T = 0.16m^{-1}$, $215.5\mu V/K$

to $-322.7\mu V/K$ at $\nabla T/T = 0.22m^{-1}$, and $278.8\mu V/K$ to $-417.6\mu V/K$ at $\nabla T/T = 0.29m^{-1}$. At $\omega_q > 2.16 \times 10^{13}s^{-1}$, the graph switched from positive to negative values of S indicating that at such frequencies, the n-type FSG changes to p-type FSG. In Fig. 4b, the S is plotted against T . Here, the diffusion depends on temperature gradient present in the material which creates the opposite field. From the graph, the S decreases with increasing T . At $\omega_q = 1.2 \times 10^{12}s^{-1}$, and $T = 77K$, the $S = 8.8\mu V/K$. By increasing the frequencies also increases the value of the Seebeck coefficient.

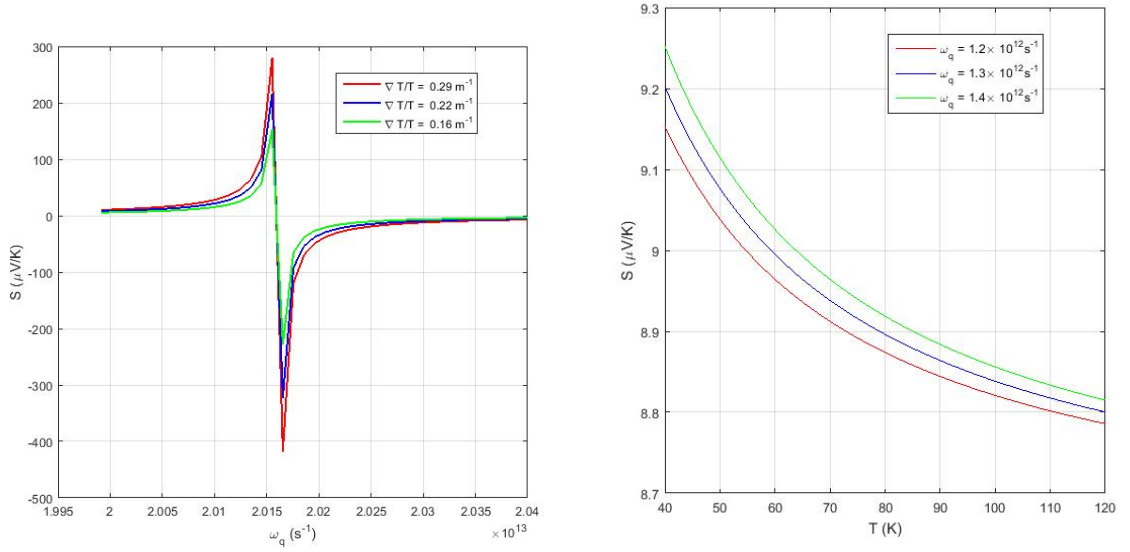


Figure 4: (left) the graph of S versus ω_q for various $\nabla T/T$ (right) the dependence of S versus T for varying ω_q

Conclusion

The influence of external temperature gradient ∇T on AE in FSG is studied. The thermal field $(\nabla T)^g$ is calculated to be $746.8 K m^{-1}$. Negative

differential conductivity ($|\frac{\partial j}{\partial T}| < 0$) is observed to manifest in FSG. The current density was calculated to be $j_T = 1.1mA\mu m^{-2}$ at $\omega_q = 0.1THz$ and the Seebeck coefficient evaluated to be $S = 8.8\mu V/K$. FSG is therefore a suitable material for the development of thermal amplifiers and logic gates.

Reference

Bibliography

- [1] Mensah, S. Y., Allotey, F. K. A., Mensah, N. G., Elloh, V. W., Amplification of acoustic phonons in a degenerate semiconductor superlattice. Physica E, Vol. 19(3) ,2003
- [2] Mensah, S. Y., Allotey, F.K.A. and Adjepong, S.K. , J. Phys.: Condens. Matter 6, (1994) 6793
- [3] Mensah, S. Y., Allotey, F.K.A. and Mensah, N.G., J. Phys.: Condens. Matter 12, (2000) 5225
- [4] Mensah, S. Y., Allotey, F.K.A. and Mensah, N.G., Akrobotu, H., Nkrumah, G., Superlattice and Microstructure 37 (2005) 87 97
- [5] Dompheh, K. A., et al. "Hypersound Absorption of Acoustic Phonons in a degenerate Carbon Nanotube." arXiv preprint arXiv:1502.07636 (2015).
- [6] Ebbecke, J., Strobl, C. J., and Wixforth, A., "Acoustoelectric current transport through single-walled carbon nanotubes", Physical Review B, APS, 2004.

- [7] Reulet, B., Kasumov, Yu. A. , Kociak, M., Deblock, R., Khodos, I. I., Gorbatov, Yu. B. , Volkov, V. T. , C. Journet and H. Bouchiat ‘Acoustoelectric Effect in Carbon Nanotubes’, physical Review letters, Vol. 85 Number 12, 25, 2000.
- [8] Dompok, K. A., N. G. Mensah, S. Y. Mensah, F. Sam, and A. K. Twum. ”Acoustoelectric Effect in degenerate Carbon Nanotube.” arXiv preprint arXiv:1504.05484 (2015).
- [9] Nghia, N. V., Bau, N. Q., Vuong, D. Q. Calculation of the Acousto-magnetoelectric Field in Rectangular Quantum Wire with an Infinite Potential in the Presence of an External Magnetic Field, PIERS Proceedings, Kuala Lumpur, MALAYSIA 772 - 777, (2012).
- [10] Cunningham, J., et al. ”Acoustoelectric current in submicron-separated quantum wires.” Applied Physics Letters 86.15 (2005): 2105.
- [11] Dompok, K. A., N. G. Mensah, and S. Y. Mensah. ”Acoustoelectric Effect in Graphene with degenerate Energy dispersion.” arXiv preprint arXiv:1505.05031 (2015).
- [12] Gulayev, Yu V. ”Acousto-electric effect and amplification of sound waves in semiconductors at large sound intensities.” Physics Letters A 30.4 (1969): 260-261.
- [13] Gurevich, V. L., R. Katilius, and B. D. Laikhtman. ”Nonlinear Amplification and Automodulation of Sound in Piezoelectric Semiconductors.” Physical Review Letters 21.24 (1968): 1632.

- [14] Gokhale, Vikrant J., Yu Sui, and Mina Rais-Zadeh. "Novel uncooled detector based on gallium nitride micromechanical resonators." SPIE Defense, Security, and Sensing. International Society for Optics and Photonics, 2012.
- [15] Fleming, W. J., and J. E. Rowe. "Acoustoelectric effects in indium antimonide." *Journal of Applied Physics* 42.5 (1971): 2041-2047.
- [16] Miseikis, V., J. E. Cunningham, K. Saeed, R. O'Rorke, and A. G. Davies. "Acoustically induced current flow in graphene." *Applied Physics Letters* 100, no. 13 (2012): 133105.
- [17] Bandhu, L. and Nash, G. R., Temperature dependence of the acoustoelectric current in graphene, *Applied Physics Letters* 105, 263106 (2014)
- [18] Balandin AA. Thermal properties of graphene and nanostructured carbon materials. *Nat Mat* 2011;10(8):56981
- [19] Sankeshwar, N. S., S. S. Kubakaddi, and B. G. Mulimani. "Thermoelectric power in graphene." *Intech* 9 (2013): 1-56.
- [20] Dompok, K. A., S. Y. Mensah, N. G. Mensah, and S. K. Fosuhene. "Thermoelectric Amplification of Phonons in Graphene." *arXiv preprint arXiv:1506.06498* (2015).
- [21] Suk, Ji Won, Karen Kirk, Yufeng Hao, Neal A. Hall, and Rodney S. Ruoff. "Thermoacoustic sound generation from monolayer graphene for transparent and flexible sound sources." *Advanced Materials* 24, no. 47, 6342-6347, 2012.

- [22] Tian, He, Tian-Ling Ren, Dan Xie, Yu-Feng Wang, Chang-Jian Zhou, Ting-Ting Feng, Di Fu et al. "Graphene-on-paper sound source devices." ACS nano 5, no. 6 (2011): 4878-4885.
- [23] B. Li, L. Wang, and G. Casati, Appl. Phys. Lett. 88, 143501 (2006).
- [24] W.-R. Zhong, P. Yang, B.-Q. Ai, Z.-G. Shao, and B. Hu, Phys. Rev. E 79, 050103 (2009).
- [25] D. He, S. Buyukdagli, and B. Hu, Phys. Rev. B 80, 104302 (2009).
- [26] E. Pereira, Phys. Rev. E 82, 040101 (2010).
- [27] D. He, B.-Q. Ai, H.-K. Chan, and B. Hu, Phys. Rev. E 81, 041131 (2010).
- [28] D. Segal, Phys. Rev. B 73, 205415 (2006).
- [29] D. M.-T. Kuo and Y.-C. Chang, Jpn. J. Appl. Phys. 49, 064301 (2010).
- [30] Daschewski, M., R. Boehm, J. Prager, M. Kreutzbruck, and A. Har-
rer. "Physics of acoustoelectric sound generation." Journal of Applied
Physics 114, no. 11 (2013): 114903.
- [31] H. Hu, Y. Wang, and Z. Wang, Wideband flat frequency response of
thermo-acoustic emission, J. Phys. D: Appl. Phys. 45, 345401 (2012).
- [32] Mariani, E., & von Oppen, F. (2008). Flexural phonons in free-standing
graphene. Physical review letters, 100(7), 076801.
- [33] Abukari, S. S., S. Y. Mensah, K. W. Adu, K. A. Dompreeh, and A. K.
Twum. "Negative Differential Conductivity in Carbon Nanotubes in the

Presence of an External Electric Field.” arXiv preprint arXiv:1101.5498 (2011).

- [34] Abukari, Sulemana S., Samuel Y. Mensah, Kofi W. Adu, Natalia G. Mensah, Kwadwo A. Dompheh, Anthony Twum, Chales LY Amuah, Matthew Amekpewu, and Musah Rabi. ”Domain Suppression in the Negative Differential Conductivity Region of Carbon Nanotubes by Applied AC Electric Field.” *World Journal of Condensed Matter Physics* 2, no. 04 (2012): 274.